International Journal of Automotive Technology, Vol. 9, No. 4, pp. 429–436 (2008)
DOI 10.1007/s12239–008–0052–3

1229–9138/2008/041–07

PERTURBATION/CORRELATION BASED OPTIMAL INTERNAL COMBUSTION ENGINE TUNING

S. LEE*

Department of Mechanical and System Design Engineering, Hongik University, Seoul 121-791, Korea

(Received 7 January 2008; Revised 31 March 2008)

ABSTRACT–This paper addresses the application of the perturbation/correlation method to optimizing the torque output of internal combustion engines. This application was inspired by observations of the limitations in current techniques of the automotive performance tuning industry. Performance issues such as errors from true optimum spark timing and fuel injector pulse width values as well as convergence were considered for optimal tuning. The ability of the system to deal with engine cycle-to-cycle variations and their effect on input parameters is also analyzed.

KEY WORDS : Internal combustion engine turning, Optimal tuning, Perturbation/Correlation

1. INTRODUCTION

Current techniques for small scale engine tuning revolve around the concept of a lookup table of fuel and spark advance versus rpm and load as generated by a technician. Typically, this table is generated through trial and error processes utilizing a combination of operator experience and dynamometer data. One major disadvantage of this method is that the operator has no indication of how close they are to the optimum settings. There are no gradient data given to indicate which parameters need to be adjusted or if they should be increased or decreased. Often only the air-fuel ratio is adjusted, as the effect of adjusting several parameters at once is beyond the skill level of the majority of operators. This assumes that torque data from a dynamometer are even available. Often technicians performing the reprogramming are misinformed as to operating conditions that produce favorable torque, such as tuning for minimizing or maximizing the wrong exhaust gasses, such as CO.

The perturbation/correlation technique will be investigated for providing a consistent automatic closed loop direct adaptive technique to engine optimization to replace the current trial and error procedures. This technique would be advantageous as it removes the operator from the loop and uses measured torque data from a dynamometer as the required feedback for updating the parameters. This method would provide enormous flexibility in its application to engines of all kinds without requiring any modification to the software or having user inputs. The values of the optimized parameters could be applied directly to the lookup table, which would allow current engine management computers to be updated without changing their basic structure.

**Corresponding author*. e-mail: sooyong@hongik.ac.kr

Much work has been performed in trying to optimize engine torque output. Many of these methods involve adaptive controls. The unknown system must be identified if indirect adaptive techniques are to be used. Typically, neural networks or fuzzy logic systems have been incorporated for the system identification role. Once a satisfactory model has been established, standard classical control schemes are used to optimize the system.

Lenz and Schroeder applied a neural network in Lenz and Schroeder (1998) to calculate the amount of fuel required to provide a given air-fuel ratio. Their neural network provided a map from engine speed and manifold air pressure inputs to the fuel mass output. Ignition control using a neural network was tried by Mueller in Mueller and Hemberger (1998). His approach trained a neural network to estimate the optimum spark timing from a data set that was quite extensive. Fuzzy logic has been applied to finding optimal fuel quantities in Jamali *et al.* (2000). This method uses a self-tuning regulator block and a parameter estimation block in the control diagram. A predictive control strategy was suggested in Sans (1998). The predictive method brings a process to a desired response over a predicted interval. Thus, the engine inputs were adjusted such that the engine output matched the desired output over the range of time specified. This method required the inverse of the engine model response during the predicted horizon. Ohyama proposed the combination of physical models of an advanced engine control system to obtain sophisticated combustion control in ultra-lean combustion, including homogeneous compression-ignition and activated radical combustion with a light load and in stoichiometric mixture combustion with a full load. Physical models of intake, combustion and engine thermodynamics were incorporated, in which the effects of residual gas from prior cycles on

intake air mass and combustion were taken into consideration in Ohyama (2001).

A parameter identification scheme using input perturbations was used in Ault *et al.* (1994). This technique used a model developed by Chang that predicts the air-fuel ratio using previous air-fuel ratios, oxygen sensor dynamics, wall wetting coefficient, and several other parameters. These parameter coefficients were identified using dithering of the throttle angle, fuel, and load. Varying these parameters in certain combinations excited the dynamics of the oxygen sensor, from which the required coefficient could be determined. Once the engine dynamics were properly estimated, an LQ controller was used to achieve the desired air to fuel ratio. In Tang *et al.* (1998), Tang discusses using perturbations of the amount of fuel injected to estimate the air-fuel ratio before the oxygen sensor has warmed up to operating temperature. However, the perturbation analysis is quite different from the perturbation/correlation method. This method was able to fairly accurately estimate the required fuel injection pulse width. This estimate successfully allowed them to use variations in fuel injection pulse width to accurately predict the air-fuel ratio of the next cycle. This value is supplied as feedback to the computer to replace the oxygen sensor output until it has warmed up to operating temperature. It does not provide a means to determine the optimum fuel injection pulse width for torque output or for any other performance index.

2. PERTURBATION/CORRELATION

Perturbation/correlation is a direct adaptive technique in which the unknown system does not need to be characterized. The output is monitored as the input is varied. Based on the behavior of the output, the inputs are adjusted towards their desired final values. Engine output is relatively easily measured using fewer sensors than would be required to train a neural network. The operating points would not wander away from the optimal values as would happen if the neural network did not fully identify a change in the condition of the engine. Currently perturbations are applied to the fuel injection for the equivalence ratio to vary from slightly lean to slightly rich. This approach is used to increase the efficiency of the catalytic converter, and it does not have any relation to the perturbation/correlation method.

The perturbation/correlation method enables the gradient of a function to be found by varying parameters in a sinusoidal fashion. The approach uses an integral correlation function, rather than a numerical derivative, which yields stability and increased insensitivity to noise in the signal.

Suppose a function of a parameter is given as $F=\Phi(x)$. A sinusoidal perturbation can be applied to the nominal operating point, x_o, that varies with time, t, at a frequency of ω.

$$x(t)=x_0+\delta_x(t) \tag{1}$$

$$\delta_x(t)=\varepsilon \sin(\omega_x t) \tag{2}$$

This perturbation yields a set of data points from which the gradient is to be determined. This perturbation is applied over one period of oscillation. The correlation term shall be defined as follows

$$R_x=\int_t^{t+2\pi/\omega_x} \delta_x(\tau)\Phi(x(\tau))d\tau, \tag{3}$$

where $2\pi/\omega_x$ is the time for a single period. This correlation can also be expressed with a summation sampled over time intervals of $t_i=\pi i/n\omega_x$, i=1,..., $2n$ replacing the integral as

$$\widehat{R}_x=\sum_{i=1}^{2n} \varepsilon \sin\left(\frac{\pi}{n}i\right)\Phi(t_i). \tag{4}$$

The slope K of the sampling of points ($x(t_i)$, $\Phi(t_i)$; i=1,..., $2n$) is given by

$$K=\frac{\sum_{i=1}^{2n}([x(t_i)-\bar{x}][\Phi(t_i)-\overline{\Phi}])}{\sum_{i=1}^{2n}(x(t_i)-\bar{x})^2}, \tag{5}$$

where $\bar{x}=\frac{1}{2n}\sum_{i=1}^{2n}x(t_i)$ and $\overline{\Phi}=\frac{1}{2n}\sum_{i=1}^{2n}\Phi(t_i)$.

(5) becomes

$$K=\frac{\sum_{i=1}^{2n}\varepsilon \sin\left(\frac{\pi}{n}i\right)[\Phi(t_i)-\overline{\Phi}]}{\sum_{i=1}^{2n}\varepsilon^2 \sin^2\left(\frac{\pi}{n}i\right)}. \tag{6}$$

Then, applying the simplifications

$$\sum_{i=1}^{2n}\overline{\Phi}\varepsilon \sin\left(\frac{\pi}{n}i\right)=0 \tag{7}$$

and

$$\sum_{i=1}^{2n}\varepsilon^2 \sin^2\left(\frac{\pi}{n}i\right)=n\varepsilon^2 \tag{8}$$

yields

$$K=\frac{\sum_{i=1}^{2n}\Phi(t_i)\sin\left(\frac{\pi}{n}i\right)}{n\varepsilon}, \tag{9}$$

Comparing this result with (4) shows that

$$\widehat{R}_x=n\varepsilon^2 K. \tag{10}$$

The correlation term is shown to represent the gradient, K, of the function at the nominal point x_o multiplied by known constants. Again, this gradient is found using only a simple integral, leading to reliable calculation of the gradient despite noisy signals.

The parameter x_o is updated based on this gradient using the following equation

$$x_{new}=x_0+\gamma\frac{\partial\Phi}{\partial x}. \tag{11}$$

By adding the second term, x is driven towards a local maximum using Newton's Method.

The derived method can be applied to two parameters having orthogonal perturbations. A function of two parameters, x and y, is given as

$$F=\Phi(x, y). \tag{12}$$

Expanding the above function yields the approximation

$$\Phi[x(\tau+\Delta t), y(\tau+\Delta t)]=$$

$$\Phi[x(\tau), y(\tau)]+\delta_x(t)\frac{\partial\Phi}{\partial x}\bigg|_\tau+\delta_y(t)\frac{\partial\Phi}{\partial y}\bigg|_\tau. \tag{13}$$

where δ_x and δ_y are perturbations along the x and y axes, respectively. Consider the perturbations being orthogonal to each other and given as $\delta_x=\varepsilon_x\sin(\omega_x t)$ and $\delta_y=\varepsilon_y\sin(\omega_y t)$. The correlation between δ_x and Φ provides

$$\bar{\delta}_x\bar{\Phi}=\int_{\tau-\frac{2\pi}{\omega_x}}^{\tau}\delta_x\Phi[x(\tau), y(\tau)]dt+$$

$$\int_{\tau-\frac{2\pi}{\omega_x}}^{\tau}\delta_x^2\frac{\partial\Phi}{\partial x}\bigg|_\tau dt+\int_{\tau-\frac{2\pi}{\omega_x}}^{\tau}\delta_x\delta_y\frac{\partial\Phi}{\partial y}\bigg|_\tau dt. \tag{14}$$

The following simplifications can be made:

$$\int_{\tau-\frac{2\pi}{\omega_x}}^{\tau}\delta_x dt=0, \tag{15}$$

$$\int_{\tau-\frac{2\pi}{\omega_x}}^{\tau}\delta_x^2 dt=\frac{\pi\varepsilon_x^2}{\omega_x}, \tag{16}$$

$$\int_{\tau-\frac{2\pi}{\omega_x}}^{\tau}\delta_x\delta_y dt=0. \tag{17}$$

Applying these to the correlation equation yields

$$\bar{\delta}_x\bar{\Phi}=\frac{\pi\varepsilon_x^2}{\omega_x}\frac{\partial\Phi}{\partial x}\bigg|_\tau. \tag{18}$$

Rewriting (18) as

$$\frac{\partial\Phi}{\partial x}\bigg|_\tau=\frac{\omega_x}{\pi\varepsilon_x^2}\bar{\delta}_x\bar{\Phi} \tag{19}$$

shows that the gradient of Φ can be determined, again using known terms of the amplitude and frequency of the perturbation of x.

To account for cycle-to-cycle variations in real engines, a random noise was introduced. This noise took the form of the absolute value of a Gaussian distribution with a 0.05 N-m standard deviation and original mean of zero. This distribution roughly describes the actual cycle-to-cycle variations as described in Heywood (1988). Also, in Fisher and Macey (1975) and Douaud and Eyzat (1977), it is shown that, under robust conditions, these distributions are close to normal distributions. Averaging the values generated by this distribution yields a Gaussian distribution according to the central limit theorem. Using the Gaussian assumption, the distribution of a given point can be expressed as

$$\psi=\bar{\psi}\pm t_v S_{\bar{\psi}}, \tag{20}$$

where ψ is the noise variable, $\bar{\psi}$ is the population average of the noises, t_v is from the student t distribution and is a function of number of samples and the confidence interval, and $S_{\bar{\psi}}$ is the averaged noise standard deviation. The Student's t-distribution (also known as t-distribution) is used because it is a probability distribution that arises in the problem of estimating the mean of a normally distributed population when the sample size is small. This can be further represented using the noise standard deviation as follows

$$\psi=\bar{\psi}+t_v\frac{S_\psi}{N^{1/2}}, \tag{21}$$

where N is the number of samples taken for the average $\bar{\psi}$. Applying noise to the perturbation/correlation equations yields

$$\Phi[x(\tau+\Delta t), y(\tau+\Delta t)]+\psi(t)=\Phi[x(\tau), y(\tau)]+$$

$$\delta_x(t)\frac{\partial\Phi}{\partial x}\bigg|_\tau+\delta_y\frac{\partial\Phi}{\partial y}\bigg|_\tau+\psi(\tau+\Delta t), \tag{22}$$

in which noise is added to the torque at time t and $t+\Delta t$. Substituting the distribution bounds for noise yields

$$\Phi[x(\tau+\Delta t), y(\tau+\Delta t)]+\bar{\psi}+t_v\frac{S_\psi}{N^{1/2}}=$$

$$\Phi[x(\tau), y(\tau)]+\delta_x(t)\frac{\partial\Phi}{\partial x}\bigg|_\tau+\delta_y(t)\frac{\partial\Phi}{\partial y}\bigg|_\tau+$$

$$\bar{\psi}+t_v\frac{S_\psi}{N^{1/2}}. \tag{23}$$

Assuming that the individual noises are acting in opposite directions yields a worst case scenario of

$$\psi(t+\Delta t)-\psi(t)=\Delta\psi=\pm 2t_v\frac{S_\psi}{N^{1/2}}. \tag{24}$$

Substituting this in yields

$$\Phi[x(\tau+\Delta t), y(\tau+\Delta t)]=\Phi[x(\tau), y(\tau)]+$$

$$\delta_x(t)\frac{\partial\Phi}{\partial x}\bigg|_\tau+\delta_y(t)\frac{\partial\Phi}{\partial y}\bigg|_\tau\pm 2t_v\frac{S_\psi}{N^{1/2}}. \tag{25}$$

Correlating δ_x and Φ gives the equation

$$\bar{\delta}_x\bar{\Phi}=\int_{\tau-\frac{2\pi}{\omega_p}}^{\tau}\delta_x\Phi[x(\tau), y(\tau)]dt+$$

$$\int_{\tau-\frac{2\pi}{\omega_p}}^{\tau}\delta_x^2\frac{\partial\Phi}{\partial x}\bigg|_\tau dt+\int_{\tau-\frac{2\pi}{\omega_p}}^{\tau}\delta_x\delta_y\frac{\partial\Phi}{\partial y}\bigg|_\tau dt+$$

$$\pm\int_{\tau-\frac{2\pi}{\omega_p}}^{\tau}\delta_x\left(2t_v\frac{S_\psi}{N^{1/2}}\right)dt. \tag{26}$$

The worst case of noise versus x perturbation would be when the noise has the same sign as δ_x throughout the integration interval. This value is

$$\int_{\tau-\frac{2\pi}{\omega_p}}^{\tau} \delta_x\left(2t_v\frac{S_\psi}{N^{1/2}}\right)dt=\pm 8\varepsilon_x t_v\frac{S_\psi}{N^{1/2}}. \quad (27)$$

After applying the simplifications described earlier, (26) becomes

$$\bar{\delta}_x\bar{\Phi}=n\varepsilon^2\frac{\partial\Phi}{\partial x}\pm 8\varepsilon_x t_v\frac{S_\psi}{N^{1/2}}. \quad (28)$$

Solving for $\frac{\partial\Phi}{\partial x}$ gives

$$\frac{\partial\Phi}{\partial x}=\frac{\bar{\delta}_x\bar{\Phi}}{n\varepsilon_x^2}\pm\frac{8t_vS_\psi}{n\varepsilon_x N^{1/2}}. \quad (29)$$

Applying this value of the gradient into the Newton's Method parameter update yields

$$x_{new}=x_{old}+\gamma\left(\frac{\bar{\delta}_x\bar{\Phi}}{n\varepsilon_x^2}\pm\frac{8t_vS_\psi}{n\varepsilon_x N^{1/2}}\right). \quad (30)$$

The effect due to the noise variation can be separated and described by

$$|\text{error}|=\gamma\frac{8t_vS_\psi}{n\varepsilon_x N^{1/2}}. \quad (31)$$

This relation gives a bound on the percentile error bound based on the student *t* distribution, the number of steps per perturbation cycle, the number of firings used in the average for each step, the amplitude of the input perturbation, and the standard deviation of the cycle to cycle variations. All of these can be considered known parameters.

The gradient is the average gradient value over the range of the perturbation of a parameter. Therefore, the applied perturbations must be small to obtain a value close to the true gradient at the nominal point. The largest updates given by $\gamma\partial\Phi/\partial x$ should be bounded reasonably small values. This condition is imposed to ensure the stability of Euler's Method. This method finds local maximums based on the Euler's Method parameter update.

3. MODELING OF THE INTERNAL COMBUSTION ENGINE FOR SIMULATION

The simulator used to calculate torque generated given a set of spark timing and equivalence ratio parameters relies on a few basic thermodynamic, geometric, fluid mechanic, and heat transfer relations. The major assumptions are that the working gases behave ideally and that the flow through the valves is quasi-static, incompressible, and one dimensional. Also, the combustion event is assumed to follow a cosine law, which is widely accepted based on experimental analysis. Even with these assumptions, the difference between calculated and measured values for the Cooperative Fuels Research Engine, on which this simulation is based, is within 5 to 10 percent--as described in Caton (1998, 2002)--because such simulations still retain most of the important features of engines. In particular, these features include time (or crank-angle) varying quantities such as the cylinder gas pressure and temperature, heat release, heat loss, intake and exhaust flow rates and cylinder mass. In addition, the basic simulation described in this paper includes parameters that vary as functions of engine speed such as combustion duration, friction, exhaust and intake manifold pressure. Table 1 and Table 2 give an overview of the variables associated with the simulator.

Table 1. Variables.

Variable	Description	Units
T	Cylinder temperature	K
V	Cylinder volume	m^3
p	Cylinder pressure	kPa
a	Crank radius	m
l	Connecting rod length	m
r	Compression ratio	Unitless
B	Cylinder bore diameter	m
$\Delta\theta$	Step size	rad
LHV	Lower heating value	kJ/kg
AF	Air to fuel ratio	Unitless
N	Engine speed	RPM
Cd	Discharge coefficient	Unitless
θ	Crank angle	rad
γ	Ratio of specific heats	Unitless
L	Stroke	m
m	Mass	kg
Vcl	Clearance volume	m^3
Vd	Displaced volume	m^3
W	Work	kJ

Table 2. Engine operating parameters.

Parameter	Value	Unit
Bore	82.6	mm
Stroke	114.3	mm
Displacement	612	cm^3
Con rod length	254	mm
Combustion duration	50	deg
Ignition delay	20	deg
Injector flow rate	3.15	g/sec
Intake valve diameter	31.75	mm
Intake valve lift	6.35	mm
Exhaust valve diameter	31.75	mm
Exhaust valve lift	6.35	mm
Engine speed	1800	RPM
Intake pressure	95	kPa
Intake temperature	313	K
Exhaust pressure	105	kPa
Exhaust temperature	600	K

The cycle is stepped through at one-degree increments and the parameters are updated using Newton's method. Therefore, all of the equations are put in the form of a derivative with respect to crank angle. The parameters are updated using the form of

$$\beta_{new}=\beta_{old}+\frac{d\beta}{d\theta}\Delta\theta, \tag{32}$$

where β is some arbitrary parameter of interest and $\Delta\theta$ is the step size in radians. The simulation begins at the Intake Valve Closing event and proceeds 720 degrees until the valve closes again. This process is completed three times to allow for the initial conditions to converge to their steady state values.

Modeling the compression and expansion strokes involved several assumptions. The first major assumption was that the fuel air mixture and combusted gas behaved ideally allowing for temperatures to be calculated using

$$T=\frac{pV}{mR}, \tag{33}$$

where p is the cylinder pressure, V is the volume, m is the mass, and R is the ideal gas constant. Along with being an ideal gas, it is assumed that the specific heats of the gas also remain constant. Cylinder pressure was updated every crank angle using the differential pressure and the Newton's Method as follows:

$$p_{new}=p_{old}+\frac{dp}{d\theta}\Delta\theta. \tag{34}$$

The differential pressure was found to be

$$\frac{dp}{d\theta}=\frac{\gamma+1}{V}\left\{\left(\frac{\delta Q}{d\theta}\right)_{net}-\left(\frac{\gamma}{\gamma-1}\right)p\frac{dV}{d\theta}+\dot{m}_{in}h_{in}-\dot{m}_{out}h_{out}\right\}, \tag{35}$$

where $d\theta$ is the angular step size, $(\delta Q/d\theta)_{net}$ is the net heat addition rate, $\dot{m}_{in}h_{in}$ represents the addition of energy due to flow in through the valves, and $\dot{m}_{out}h_{out}$ is the loss of energy out of the valves. This relation was derived from a balance of internal energy

$$\frac{d(mu)}{d\theta}=\left(\frac{\delta Q}{d\theta}\right)_{net}-p\frac{dV}{d\theta}+\dot{m}_{in}h_{in}-\dot{m}_{out}h_{out}, \tag{36}$$

in which u is the internal energy of the cylinder contents. The cylinder volume is constrained geometrically by the cylinder, crank, and connecting rod dimensions as well as the crank angle as shown in

$$V(\theta)=V_{cl}+\frac{\pi B^2}{4}[l+a-a\cos\theta-\sqrt{l^2-a^2\sin\theta}], \tag{37}$$

where l is the connecting rod length, a is the crank radius, B is the cylinder bore, and V_{cl} is the clearance volume at top dead center. This is not a purely simple sinusoidal function due to the connecting rod and crank linkage geometry. Again, the rate of change of volume with respect to θ is of interest and is calculated to be

$$\frac{dV}{d\theta}=\frac{\pi B^2}{4}a\sin\theta\left(1+\frac{\cos\theta}{\sqrt{\left(\frac{l}{a}\right)^2-\sin^2\theta}}\right), \tag{38}$$

Heat is assumed to be transferred through the cylinder wall surface area as convection, with the wall temperature being a constant. This condition is due to the large thermal mass of the metal walls and coolant system in relation to the rate of temperature change of the gas. The convective heat transfer coefficient had been experimentally established in Heywood (1988) and Woschini (1967) as

$$h_{conv}(\theta)=2.446\times10^{-4}\left(\frac{2aN}{30}\right)^{1/3}[p(\theta)T(\theta)]^{1/2}, \tag{39}$$

where a is the crank radius and N is the engine revolutions per minute with a correction factor of α=9.549/N to give units of kW/m^{2}K×rad. The cylinder surface area as a function of crank angle is given as

$$A(\theta)=\frac{2\pi B^2}{4}+\frac{4V_{cl}}{B}+\pi B[l+a-a\cos\theta-\sqrt{l^2-a^2\sin^2\theta}], \tag{40}$$

which represents the surface area of the piston crown, clearance volume, and the walls of a right cylinder exposed as the piston moves down. The rate of heat loss or gain is given by the relation

$$\left(\frac{dQ}{d\theta}\right)_{heat}=h_{conv}A(\theta)(T_{wall}-T), \tag{41}$$

where T_{wall} is the constant wall temperature. This yields a relation of heat loss or gain as a function of crank angle, which falls in line with what is required by the simulation method.

The combustion process was modeled using a cosine law, as it exhibits slow combustion during the beginning and end of the combustion process because of the small flame front area. It also shows a faster rate in between since the flame front is large and consumes the fuel and air mixture quickly. The rate of heat release is of interest in the simulation and can be represented as

$$\frac{dQ}{d\theta}=\frac{LHV(M_{fuel})\pi\sin\left(\pi\frac{\theta-\theta_0}{\theta_b}\right)}{2\theta_b}, \tag{42}$$

where LHV is the lower heating value of the fuel, M_{fuel} is the mass of fuel in the cylinder, θ_b is the combustion duration, and θ_o is the start of combustion. This equation is valid for EQ<1, which is the excess air condition. The equivalence ratio can be calculated using

$$EQ=14.7\frac{M_{fuel}}{M_{air}}, \tag{43}$$

For mixtures with excess fuel, the amount of heat released is dependent on the air available to be burnt. The equation

describing this condition is as follows:

$$\frac{dQ}{d\theta}=\frac{LHV\left(\frac{M_{air}}{14.7}\right)\pi\sin\left(\pi\frac{\theta-\theta_0}{\theta_b}\right)}{2\theta_b}, \tag{44}$$

where M_{air} is the mass of air in the cylinder as calculated from

$$M_{air}=m-M_{fuel}, \tag{45}$$

where m is the total mass of cylinder contents. The mass of fuel delivered to the cylinder is quantified as

$$M_{fuel}=\dot{Q}_{inj}t_{inj}, \tag{46}$$

in which $\dot{Q}_{inj}$ is the fuel injector flow rate in kilograms per second and t_{inj} is the time the fuel injector is held open in seconds. This analysis assumes that the flow rate is constant and the injector achieves this rate immediately upon opening. Also, it is assumed that the entire mass of fuel injected is combusted during that cycle.

The combustion process is begun by a spark, but there is a delay before combustion begins, known as the combustion delay. Therefore, θ_o is the angle at which the spark is initiated plus the combustion delay. This heat release model assumes that the heat is uniformly distributed as the combustion event occurs and the fuel and air mixture is homogenous. The flow through the valves is assumed to be quasi-steady flow, one-dimensional, reversible, adiabatic, incompressible and with constant discharge coefficients. The flow area is assumed to be the curtain area between the circumference of the valve and the valve seat. This relation can be expressed as

$$A_{throat}=C_d\pi D_v L(\theta), \tag{47}$$

where C_d is the discharge coefficient, D_v is the valve diameter, and $L(\theta)$ is the instantaneous valve lift. The cam profile is assumed to be sinusoidal throughout its entire duration, so the lift equation takes the form of

$$L(\theta)=L_{\max}\sin\left\{\pi\frac{\theta-\theta_{vo}}{\theta_{dur}}\right\}, \tag{48}$$

where $L_{\max}$is the maximum lift, θ_{vo} is the valve opening angle, and θ_{dur} is the duration of opening. This relation is used only when θ is bounded by the opening and closing angles; otherwise, the lift is assumed to be zero. The flow into or out of the cylinder can be either sonic (choked) or subsonic depending on the ratio of the throat pressure compared to the upstream pressure. If the inequality

$$\frac{p_u}{p_t}\geq\left(\frac{\gamma+1}{2}\right)^{\gamma/\gamma-1} \tag{49}$$

holds true, then flow is sonic, and the maximum mass flow rate has been achieved. This mass flow rate is given by

$$\dot{m}=A_t p_u\sqrt{\frac{\gamma}{RT_u}\left(\frac{2}{\gamma+1}\right)^{(\gamma+1)/(\gamma-1)}}, \tag{50}$$

where A_t is the throat area, and p_u and T_u are the upstream pressure and temperature, respectively. If the flow is subsonic, then the following relation gives the mass flow rate

$$\dot{m}=A_t p_u\sqrt{\frac{2}{RT_u}\left(\frac{p_t}{p_u}\right)^{2/\gamma}\frac{\gamma}{\gamma-1}\left[1-\left(\frac{p_t}{p_u}\right)^{(\gamma-1)/\gamma}\right]}. \tag{51}$$

p_t is the pressure at the restriction or throat, and the flow rate is in kilograms per second. The same factor, a, from the heat transfer section is used in converting the flow rate from kilograms per second to kilograms per radian. The total mass contained within the cylinder was found using conservation of mass principles and Newton's method as shown in

$$m_{new}=m_{old}+(\dot{m}_{in}-\dot{m}_{out})\Delta\theta. \tag{52}$$

Friction is caused by rubbing in the bearings between the connecting rod and crankshaft, the cam on the tappet, the piston rings sliding against the cylinder walls, as well as the crank rotating on the main bearings. In Heywood (1988), this energy loss due to friction can be expressed as an equivalent pressure using the experimentally derived relation of

$$FMEP_{total}=94.8+2.3\left(\frac{N}{1000}\right)+4.0\left(\frac{N}{1000}\right)^2, \tag{53}$$

where *FMEP* is the friction mean effective pressure in kPa and N is the engine speed in revolutions per minute. This relation indicates that friction increases significantly as engine speed increases.

The parameter of interest to be derived from the simulation is torque. Using the brake mean effective pressure as calculated using

$$BMEP=IMEP–FMEP, \tag{54}$$

where *IMEP* is the indicated mean effective pressure, an indication of torque output can be gathered. *IMEP* is the net amount of pressure generated by the gas, and it can be calculated by analyzing the work done on the cylinder at each time step. The equation for the work done is

$$W_{net}=\Sigma(p-FEMP)\frac{dV}{d\theta}\Delta\theta, \tag{55}$$

where p is the cylinder pressure, $dV/d\theta$ is the rate of change of volume with respect to angle, and $\Delta\theta$ is the incremental change in angle. The negative work done by compressing the gas and positive work done by the expanding gas is taken care of by the sign of $dV/d\theta$. From the work calculation, *BMEP* can be found using

$$BMEP=\frac{W_{net}}{V_d}. \tag{56}$$

The torque generated by this pressure can be calculated for the four stroke cycle engine by the relation

$$\tau=1000\frac{BMEP\cdot V_d}{4\pi}, \tag{57}$$

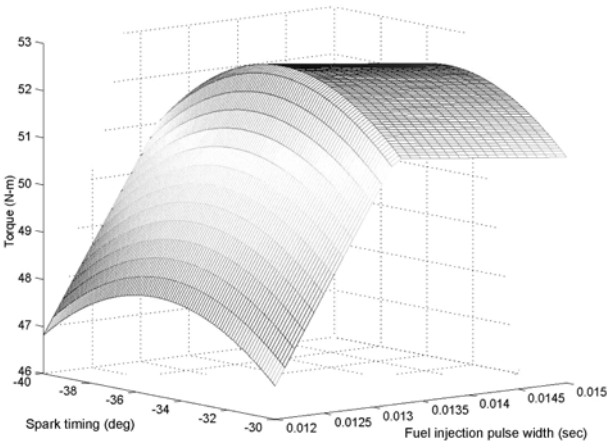

Figure 1. Torque contour.

where t is the net torque in Newton-meters generated by the engine and V_d is the displaced volume of the engine.

4. SIMULATION RESULTS

To get a better understanding of the system characteristics, a plot of torque over the entire range of spark timings and equivalence ratio was made, as shown in Figure 1. Spark timing and fuel injection pulse width are the two input parameters. By updating these two parameter values the torque output is maximized. Two inputs are perturbed concurrently with orthogonal periodic functions.

This plot shows that the torque is very sensitive to changes in spark timing as well as lean operation. Not much change is evident when the engine is running rich. The contour also has the important feature of having only one local maximum. This characteristic alleviates the problem of the perturbation's finding a local maximum that is not the global maximum. The values of interest for the maximum are a spark timing of 35 degrees before top dead center, 13.3 milliseconds of fuel injection pulse width, and the resulting output torque is 52.65 Newton meters. The torque output, optimal spark timing, and fuel injection pulse width are insensitive to changes in engine speed. This result clearly shows that the engine does not need to be held at a precise speed during the tuning process. The shape of the torque contour remains the same over this range as well. The spark timing was quantized at 0.5 degrees, and the fuel pulse at 0.05 milliseconds, to ensure compatibility with a wide range of engine management computers. The amplitude of the spark perturbation was set at 0.5 degrees, and the fuel was set at 0.05 milliseconds with 5 steps per perturbation cycle. These amplitudes were chosen to keep the evaluation of the gradient as close to a single point as possible given the constraints listed above.

The input parameter updates after each perturbation/correlation cycle are shown in Figure 2. The top left figure shows how the spark timing changes after each perturbation cycle. The bottom left figure depicts the size of each

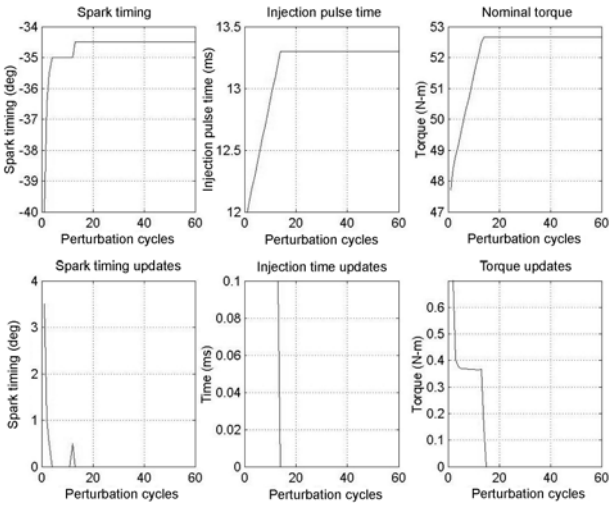

Figure 2. Input values and update sizes over time.

change in spark timing. The top middle figure shows the fuel injection pulse width after each perturbation cycle. The bottom middle plot shows the size of the change in fuel injection pulse width. The top right plot shows the torque generated by the spark timing and fuel injection pulse width for each perturbation cycle. The bottom right figure shows how much the torque changes over each cycle. The fuel injection pulse timing oscillates slightly, primarily because of the sharp change in the shape of the torque versus equivalence ratio contour. The amplitude of the oscillation is small enough that it has a minimal effect on the output torque, as illustrated in the torque update portion of Figure 2.

The following figure shows the results of this arrangement in topographical map. The initial conditions of spark timing and fuel injection pulse width were –40 degrees

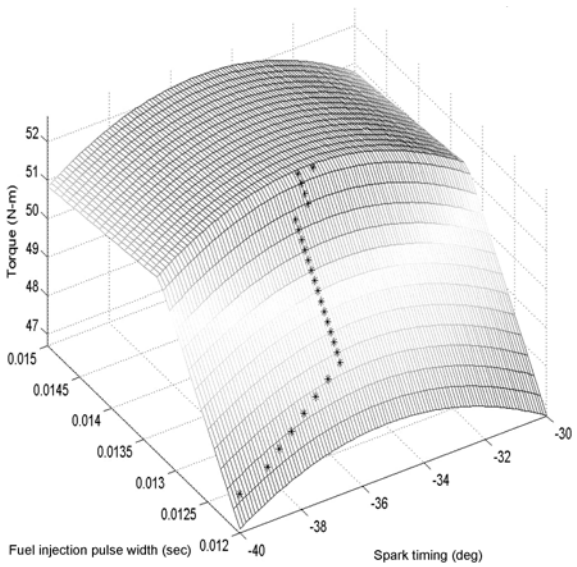

Figure 3. Performance contour illustrating input parameter paths.

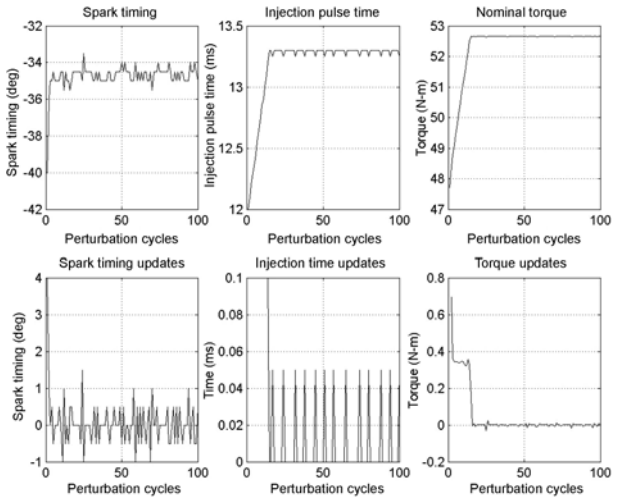

Figure 4. Five percent noise with 200 firings per perturbation.

before top dead center and 12 milliseconds, respectively. Each star on the plot represents the torque value after each perturbation cycle. They start at the bottom corner and move up the contour towards the peak, where it settles into its steady state values. This figure shows how the torque values climb up the contour to the maximum. Examining a topographical map of the contour gives a clearer indication the gradients of the torque contour.

To simulate true operating conditions, variations in the torque were added to the nominal torque value produced by the simulator. The noise was given as a Gaussian distribution with a zero mean and initial standard deviation of one. The simulator represented the best case of combustion, so the positive values of the random torque underwent a sign change. To determine the robustness of the perturbation/correlation method, the multiplier on the random inputs was varied to add on average approximately 5 percent of the maximum nominal torque value. Figure 4 shows the effect of a noise on the output torque measurement.

The stability is reduced, but the spark timing and injection pulse width updates are still within a reasonable bound. Again, the variation in the output torque due to the constantly changing input parameters is minimal. Any more noise would increase the variation of spark timing and injection pulse width per perturbation cycle to beyond an acceptable limit. The effect of the noise on the nominal output torque has been eliminated. There is still a slight variation in the input parameters, but it has essentially converged.

5. CONCLUSION

This method can be used to optimally tune engines automatically with no human input required. An engine can be quickly optimized with very little variation in the final parameters over time, given little to no noise since the algorithm always converges to the maximum output torque.

Significant cycle-to-cycle variations can be tolerated by modifying the number of firings per step as prescribed in the no noise case. This robustness comes at the expense of reducing the convergence time. This direct adaptive tuning method is advantageous compared to existing methods for custom tuners since it requires very few parameters to be known about the engine to be tuned and since it can be very tolerant of cycle to cycle variations.

ACKNOWLEDGEMENT–This work was supported by 2005 Hongik University Research Fund.

REFERENCES

Ault, B., Jones, V. K., Powell, J. D., and Franklin, G. F. (1994). Adaptive air-fuel ratio control of a spark ignition engine. *SAE Paper No.* 940373.

Caton, J. A. (1998). Development and use of a basic thermodynamic cycle simulation for commercial automotive spark-ignition engines. *Proc. 1998 Central States Section/Combustion Institute Spring Technical Meeting*, *Paper No.* 98-06, 29–34.

Caton, J. A. (2002). Illustration of the use of an instructional version of a thermodynamic cycle simulation for commercial automotive spark-ignition engine. *Int. J. Mechanical Engineering Education* **30**, **4**, 283–297.

Douaud, A. and Eyzat, P. (1977). DIGITAP - An on-line acquisition and processing system for instantaneous engine data - applications. *SAE Paper No.* 770218.

Fisher, R. V. and Macey, J. P. (1975). Digital data acquisition with emphasis on measuring pressure synchronously with crank angle. *SAE Paper No.* 750028.

Heywood, J. (1988). *Internal Combustion Engine Fundamentals*. McGraw-Hill. New York.

Jamali, M., Ghandakly, A. A., and Al-Olimat, K. S. (2000). Adaptive air-fuel ratio control of an SI engine using fuzzy logic parameters evaluation. *SAE Paper No.* 2000-01-1246.

Lenz, U. and Schroeder, D. (1998). Air-fuel ratio control for direct-injecting combustion engines using neural networks. *SAE Paper No.* 981060.

Mueller, R. and Hemberger, H.-H. (1998). Neural adaptive ignition control. *SAE Paper No.* 981057.

Ohyama, Y. (2001). Engine control using combustion model. *Int. J. Automotive Technology* **2**, **2**, 53–62.

Sans, M. (1998). Global predictive and optimal control applied to automotive engine management. *SAE Paper No.* 981058.

Tang, X., Asik, J. R., Meyer, G., and Samson, R. G. (1998). Optimal A/F ratio estimation model (Synthetic Uego) for SI egine cold transient AFR feedback control. *SAE Paper No.* 980798, 1998.

Woschini, G. (1967). Universally applicable equation for the instantaneous heat transfer coefficient in the internal combustion engine. *SAE Paper No.* 670931.